Molecular Crystals and Liquid Crystals Science and Technology. Section A. Molecular Crystals and Liquid Crystals

Publication details, including instructions for authors and subscription information:
http://www.tandfonline.com/loi/gmcl19

Interfacial Ordering in a Liquid Crystal Near the Nematic - Isotropic Transition

Thomas Moses [a]

[a] Department of Physics, Knox College, Galesburg, IL, 61401

Version of record first published: 04 Oct 2006

To cite this article: Thomas Moses (1998): Interfacial Ordering in a Liquid Crystal Near the Nematic - Isotropic Transition, Molecular Crystals and Liquid Crystals Science and Technology. Section A. Molecular Crystals and Liquid Crystals, 319:1, 121-136

To link to this article: http://dx.doi.org/10.1080/10587259808045653

Mol. Cryst. Liq. Cryst., Vol. 319, pp. 121 – 136
Reprints available directly from the publisher
Photocopying permitted by license only

Interfacial Ordering in a Liquid Crystal Near the Nematic – Isotropic Transition

THOMAS MOSES

Department of Physics, Knox College, Galesburg, IL 61401

(Received 10 December 1997; In final form 19 March 1998)

The molecular ordering of the liquid crystal 8CB near a surfactant-coated glass surface has been studied using evanescent-wave ellipsometry. Surface molecular ordering was measured in the isotropic phase, and both bulk and surface ordering were measured simultaneously in the nematic phase in the vicinity of the nematic–isotropic transition temperature T_{NI}. Two kinds of behavior were observed, depending on the strength of the surface-liquid crystal interaction in a given sample. (1) For samples with a strong surface-liquid crystal interaction, at temperatures above T_{NI} the interface is wet by a homeotropically oriented, ordered layer whose thickness diverges as the temperature T approaches T_{NI}. For $T < T_{NI}$, the interface is wet by an surface region of enhanced nematic order whose thickness increases as $T \rightarrow T_{NI}$ but remains finite at T_{NI}. (2) For samples with a weak surface-liquid crystal interaction, at temperatures above T_{NI} the interface is wet by an ordered layer whose thickness increases but remains finite as $T \rightarrow T_{NI}$. For $T < T_{NI}$, the interface is wet by a disordered surface region whose thickness increases but remains finite as $T \rightarrow T_{NI}$. The results are analyzed in terms of the Landau-de Gennes theory and found to be in qualitative agreement with theoretical predictions.

Keywords: Interfacial ordering; surface ordering; nematic–isotropic transition; ellipsometry; liquid crystal interface

PACS: 61.30.Gd, 64.70.Md, 68.45.Gd

1. INTRODUCTION

Molecular ordering in liquid crystals (LCs) in the vicinity of a substrate surface has been a problem of long-standing interest to liquid crystal researchers. The first investigations probed nematic surface order in the isotropic phase of LCs. It was found that surfaces specially treated to align the bulk nematic phase generally induce enhanced surface ordering in the

adjacent LC layer at temperatures where the bulk is isotropic [1–5]. Surfaces treated with a surfactant that induces random planar orientation in the nematic phase were observed to induce an ordered layer with negative surface order parameter in the isotropic phase [2, 6]. The findings of these experiments were well described by the phenomenological Landau-de Gennes (L-dG) theory, first extended to describe surface ordering by Sheng and subsequently by others [7–11]. The findings are most readily described in terms of the adsorption parameter $\Gamma = \int_0^\infty (Q(z) - Q_B)\, dz$, where $Q(z)$ is the scalar order parameter at a distance z from the substrate and Q_B is the order parameter in the bulk. L-dG theory predicts and experiments have verified the existence of two classes of surface ordering behavior: complete wetting of the surface by an orientationally ordered layer with Γ diverging as the temperature T approaches the transition temperature T_{NI}, and partial wetting with Γ increasing but remaining finite at $T = T_{NI}$. Besides ordering near a planar substrate, surface ordering has been studied recently in a variety of different systems. The surface ordering at the free surface of an isotropic liquid crystal has been investigated [12–14]. More recently, surface-induced ordering and interesting finite-size effects on the isotropic–nematic transition have been reported in porous glass [15]. Layer-by-layer surface ordering transitions in smectic phases have also been a subject of recent experimental and theoretical interest [16].

The experimental picture of interfacial ordering on the nematic side of the isotropic–nematic transition is less clear than on the isotropic side. Several experimental studies have investigated interfacial ordering in the nematic phase and its relation to the surface anchoring energy [17–21]; these studies are reviewed in an article by Yokoyama [22]. One challenge for experiments probing nematic phase surface ordering is to discriminate a small signal due to surface ordering from the large signal due to nematic bulk ordering. The evanescent-wave ellipsometry technique allows the measurement of an optical phase shift that depends only on the *excess* birefringence of the surface layer over the bulk birefringence and vanishes when surface and bulk birefringences are equal, thus providing a direct probe of the interfacial molecular ordering. As a side benefit, the critical angles for total internal reflection can be monitored during the experiment, allowing the bulk birefringence (and thus the bulk order parameter) to be measured separately from the surface birefringence. Using evanescent-wave ellipsometry, Moses and Shen have studied interfacial ordering in the nematic phase for a SiO-coated surface inducing disorder in the adjacent region of liquid crystal [19]. Recently, Kasten and Strobl have studied the related problem of surface ordering at the free surface of a nematic liquid crystal using reflection

ellipsometry [14]. They found enhanced surface ordering by a homeotropically oriented layer in both the isotropic and nematic phases.

The purpose of this experiment is to study interface-induced order in the vicinity of the nematic–isotropic phase transition in both the nematic and isotropic phases of a liquid crystal. The evanescent-wave ellipsometry technique was used since it allows both the bulk and surface order to be monitored separately in the same experiment. Fitting surface ordering data for both the isotropic and nematic phases simultaneously provides a considerably more stringent test of the L-dG theory than earlier studies in the isotropic phase alone could provide. The system investigated was the liquid crystal 4′-cyano-4-*n*-octylbiphenyl (8CB) near a glass substrate which was coated with the surfactant *n*,*n*-dimethyl-*n*-octadecyl-3-aminopropyltrimethoxysilyl chloride (DMOAP). This system was chosen because its surface ordering behavior in the isotropic phase has been well characterized by previous experiments, where the surface was shown to be completely wet by a homeotropically oriented nematic layer [5]. L-dG theory predicts that this system should exhibit enhanced nematic surface ordering in the nematic phase, which was in fact observed. It was also observed that some samples exhibited partial wetting of the interface rather than complete wetting in the isotropic phase, evidencing a relatively weaker surface LC interaction. For such samples, surface disordering in the nematic phase was observed, again in qualitative agreement with the predictions of L-dG theory.

2. LANDAU-DE GENNES THEORY OF SURFACE ORDERING

L-dG theory has been shown to be successful in accounting quantitatively for pretransitional surface ordering in the isotropic phase and may be expected to provide a qualitatively correct description of pretransitional surface ordering in the nematic phase in the vicinity of the transition temperature [1–6, 19]. The L-dG theory of surface ordering is briefly reviewed in this section. A fuller discussion of the results presented here may be found in Refs. [2] and [7]. According to L-dG theory, the free energy density f of the LC is given by

$$f = \frac{1}{2}a(T - T^*)Q^2 - \frac{1}{3}bQ^3 + \frac{1}{4}cQ^4, \tag{1}$$

where Q is the scalar order parameter and a, b, c and T^* are material-dependent constants. Near an interface, Q may depend on the distance z

from the interface as well as on the temperature T. A term of the form $L(dQ/dz)^2$ is added to account for the free energy cost of spatial variation of the order parameter near an interface, with L a material-dependent constant. The values used for 8CB, taken from previous experiments, were $a = 2.20 \times 10^5 \text{Jm}^{-3}\text{K}^{-1}$, $b = 2.31 \times 10^6 \text{Jm}^{-3}$, $c = 4.16 \times 10^6 \text{Jm}^{-3}$, and $L = 4.5 \times 10^{-12} \text{Jm}^{-1}$ [23]. The value of T^* is obtained from $T^* = T_{\text{NI}} - (2b^2/9ac)$ with T_{NI} determined experimentally. Following Ref. [10], the free energy density f_0 associated with the interface-LC interaction is given by

$$f_0 = \left(-g Q_0 + \frac{1}{2} U Q_0^2\right) \delta(z), \tag{2}$$

where g and U are constants dependent on the LC and the nature of the interface, Q_0 is the order parameter at the interface, and the delta function represents a short-range interaction with the interface located at the plane $z = 0$. Equation (2) may be thought of as a Landau expansion for the interfacial free energy and may lead to enhanced or reduced interfacial order depending on the sign of g and the relative magnitudes of g and U. For a sample that is semi-infinite in the z direction and uniform in the x and y directions, the total free energy per area F is given by

$$F = \int_0^\infty dz \left(f + L\left(\frac{dQ}{dz}\right)^2 + f_0\right). \tag{3}$$

By minimizing the free energy F using the calculus of variations, one finds the order parameter $Q(z, T)$. In the isotropic phase, the result is

$$Q(z, T) = \frac{2a(T - T^*)Z}{(Z + (b/3))^2 - (1/2)ac(T - T^*)}, \tag{4}$$

where

$$Z = \frac{1}{Q_0}\Big(a(T - T^*) - (b/3)Q_0 + 2((a/2)(T - T^*))^{1/2} \\ (f(Q_0)/Q_0^2)^{1/2}\Big) \exp(z/\xi), \tag{5}$$

Q_0 is the order parameter at $z = 0$, and the correlation length ξ is defined by

$$\xi = \left(\frac{2L}{a(T - T^*)}\right)^{1/2}. \tag{6}$$

In the nematic phase, the order parameter is given by Eqs. (4)–(6) with $a \rightarrow a'$, $b \rightarrow b'$, $Q_0 \rightarrow Q_0 - Q_B$, and $Q(z, T) \rightarrow Q(z, T) - Q_B$ where Q_B is the order parameter in the bulk LC,

$$a' = a(T - T^*) - 2bQ_B + 3cQ_B^2, \tag{7}$$

and

$$b' = b - 3cQ_B. \tag{8}$$

Ordinarily, the order parameter $Q(z)$ described in Eqs. (4)–(6) (or the corresponding equations appropriate for the nematic phase case) differs from its bulk value Q_B only in a region near the interface of characteristic length-scale ξ. However, in the isotropic phase, for a range of surface free energy parameters g and U that result in sufficiently large Q_0, the order parameter $Q(z)$ will differ from its bulk value of zero in a region much larger than ξ at temperatures close to T_{NI}, with the length-scale of the surface layer diverging as $T \rightarrow T_{NI}$. This phenomenon occurs if $Q_0(T_{NI})$ is larger than the threshold value $Q_c = (2b/3c)$, and in this case the interface is said to be completely wet by the ordered surface layer. An analogous complete wetting phenomenon is predicted in the nematic phase for surface parameters g and U leading to $Q_0(T_{NI}) \leq 0$.

To complete the description of the order parameter profile, it is necessary to investigate how the surface free energy parameters g and U determine Q_0. Following Sheng's treatment in Ref. [7], Q_0 is determined by minimizing the boundary layer free energy per unit area given by

$$F_{BL} = f_0(Q_0) + 2\int_0^\infty dz[f(Q) - f(Q_B)], \tag{9}$$

from which, after some manipulation, follows the condition

$$0 = \pm 2L^{1/2}[f(Q_0) - f(Q_B)]^{1/2} + \frac{df_0(Q_0)}{dQ_0}, \tag{10}$$

where the positive sign holds when $Q_0 > Q_B$ and the negative sign holds in the opposite case. Using the L-dG expression for $f(Q)$ given in Eq. (1) and the form of $f_0(Q_0)$ given in Eqs. (2), (10) turns out to be a quartic polynomial in Q_0. The real root of the quartic polynomial that minimizes the boundary layer free energy F_{BL} is the desired Q_0.

The procedure for determining the order parameter profile $Q(z)$ is as follows. For a given choice of the model parameters g and U, one solves

Eq. (10) to determine the surface order parameter Q_0. In case there are multiple real roots of Eq. (10), the root that minimizes the boundary layer free energy in Eq. (9) is selected. Then the order parameter profile $Q(z)$ is given by Eqs. (4) – (6) when $T > T_{NI}$, or by the corresponding relations in the nematic phase.

3. EXPERIMENTAL APPARATUS

The evanescent-wave ellipsometry apparatus used in this work is similar to the one described in detail in Ref. [4]. The apparatus is shown schematically in Figure 1. Light from a HeNe laser is polarized, reflected from the glass-LC interface, analyzed by a polarizer orthogonal to the initial polarizer, and detected with a silicon photodiode. The LC sample is a thin film confined between a high-refractive-index glass prism (Schott glass LaSF 18A, $n = 1.85$) and a glass plate. The angle of incidence can be varied by rotating the sample assembly and detection arm, and in most experiments the angle of incidence is chosen just short of the first critical angle for total internal reflection at the glass-LC interface. Upon reflection from the glass-LC

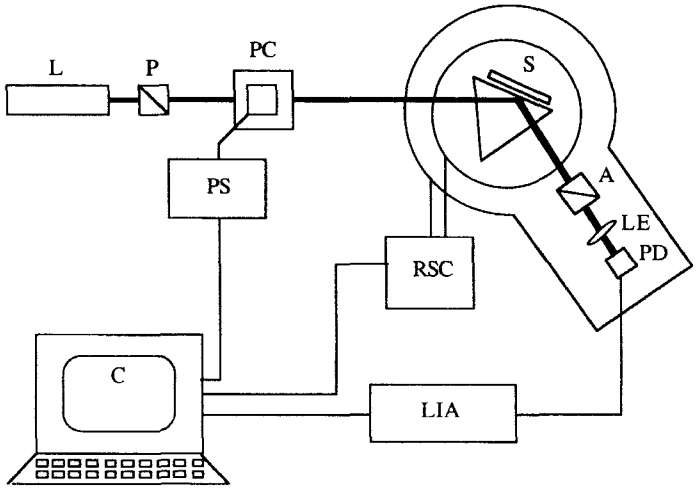

FIGURE 1 A schematic diagram of the evanescent-wave ellipsometry apparatus. L = HeNe laser, P = polarizer, PC = Pockels cell, S = temperature-controlled LC sample on rotation stage, A = analyzer, LE = lens, PD = silicon diode photodetector, PS = high voltage power supply and modulation power supply for Pockels cell, LIA = lock-in amplifier, RSC = rotation stage controller, C = computer.

interface, orthogonal *p*- and *s*-polarized components of the light are shifted in phase. This phase shift $\Delta\phi_c$ depends on both the thickness of the ordered interfacial layer in the LC and on the difference in the birefringence of the interfacial layer and the bulk medium. A Pockels cell is used to induce an equal and opposite phase shift to the one induced by the sample so that light reflected from the sample is restored to linear polarization and extinguished by the analyzer. Modulation of the Pockels cell voltage at 10 kHz allows for ac detection of the signal with a lock-in amplifier. To enhance stability of the apparatus, the Pockels cell was housed in a temperature-controlled chamber with a temperature stability of ± 0.02°C. The apparatus can resolve phase shifts as small as 0.1 mrad and drifts less than 0.5 mrad in 12 h.

The nematic LC sample is shown schematically in Figure 2. Light is incident on the prism with equal *p*- and *s*-polarized components. Since the nematic director lies normal to the substrate in the plane of incidence, *p*- and *s*-polarizations are eigenpolarizations for this geometry. In this case, the phase shift $\Delta\phi_c$ at the first critical angle vanishes if the LC medium is uniform, and a non-zero value of the phase shift $\Delta\phi_c$ indicates that the birefringence varies with distance from the interface. Roughly speaking, the larger the length-scale of the interfacial region or the greater the birefringence difference between surface and bulk, the larger the phase shift $\Delta\phi_c$. The prism and plate are separated by mylar spacers. It was found convenient to use wedged LC films so that the beam reflected from the back glass surface could be discriminated. The wedge angle was fixed at 0.7° with a minimum sample thickness of 50 μm. Since the sample thickness is

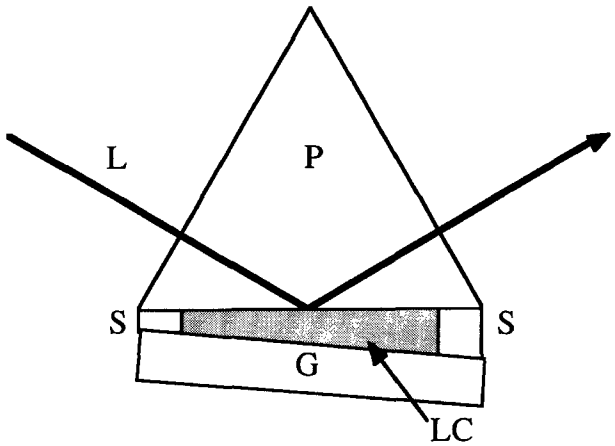

FIGURE 2 A schematic diagram of the LC sample cell. P = glass prism, LC = liquid crystal sample, G = glass plate, L = laser beam, S = mylar spacers.

much larger than the optical wavelength, the sample is effectively semi-infinite. Calculations were made to verify that the slight bend induced in the director configuration by the wedge could be neglected in the data analysis.

4. SAMPLE PREPARATION

A glass prism and glass plate were coated with the surfactant DMOAP, using the method described in Ref. [24]. Prior to the coating, glass substrates were carefully cleaned using detergent, ultrasonication in acetone, and finally soaking in concentrated chromic acid. In some cases an additional cleaning step of soaking in a potassium hydroxide solution was used before the final acid cleaning. The LC was introduced into the sample cell by capillary action while in the isotropic phase. The liquid crystal 8CB was obtained from EM industries and used without further purification. Samples were verified to be homeotropically aligned and defect-free by observation under a polarizing microscope. The assembled sample was placed in the inner chamber of a custom-built, two-stage oven with a temperature stability of $\pm 0.001°C$.

It was found that while all samples prepared under these conditions were defect-free monodomains, the samples differed in their ability to induce interfacial ordering. In the isotropic phase, Sample A exhibited complete wetting of the interface by a nematic layer, while Sample B exhibited partial wetting. In the nematic phase, Sample A exhibited enhanced nematic ordering at the interface, while Sample B exhibited reduced nematic ordering. Each sample gave consistent and reproducible results in repeated measurements. Several samples were made using slightly different substrate cleaning procedures and different batches of 8CB and DMOAP; in all cases the results were as described above, with either type A or type B interfacial ordering behavior. It appears that the above-described method of sample preparation yields samples of varying interfacial properties, perhaps due to the effects of trace surface contamination, although all samples induce defect-free nematic alignment and the interfacial properties of a given sample are stable.

5. EXPERIMENTAL RESULTS

Figure 3 shows the phase shift $\Delta\phi(\theta)$ as a function of the angle of incidence θ for a nematic sample. Note that there are two critical angles, visible as

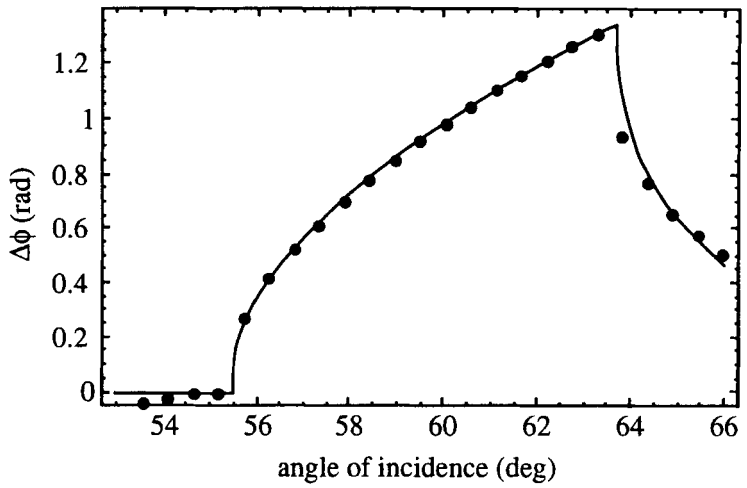

FIGURE 3 Phase shift $\Delta\phi$ *vs.* angle of incidence θ at the glass-LC interface, at fixed temperature $T = 37°C$ in the nematic phase. The solid line is a theoretical fit to the data.

discontinuities in the slope of the $\Delta\phi$ *vs.* θ curve, involving the total internal reflection of the *p*- and *s*-polarization states. As noted earlier, in this geometry the phase shift $\Delta\phi_c$ at the first critical angle for total internal reflection provides a measure of the excess surface birefringence. The solid line in the figure is a theoretical curve calculated using the known index of refraction of the glass prism and the measured indices of refraction of the nematic LC. Since the penetration depth of the evanescent wave is much larger than the interfacial layer thickness, the critical angles for total internal reflection depend only on the optical properties of the bulk medium and the indices of refraction are given by Snell's law

$$n_i = n_p \sin \theta_i \tag{11}$$

where n_p is the prism's refractive index, $i = e$ or o for the extraordinary or ordinary ray, and $\theta_o(\theta_e)$ is the smaller (larger) critical angle. The smaller critical angle corresponds to total internal reflection of the *s*-polarization and is determined by n_o. In this and subsequent theoretical curves, a small constant phase shift representing residual strain birefringence in the optics was added to the calculated values $\Delta\phi$ in order to optimize the fit.

Figure 4 shows the temperature-dependence of the bulk order parameter. The bulk order parameter was calculated in the following way. First, the critical angles for total internal refraction of the nematic were measured as

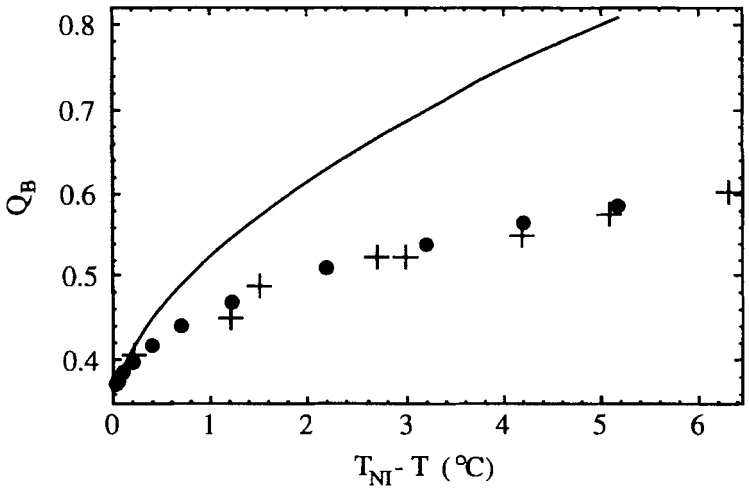

FIGURE 4 Bulk order parameter Q_B *vs.* temperature. The circles are data points, the crosses are data taken from Ref. [24], and the solid line is the L-dG theoretical curve. The L-dG curve matches the experimental data within 10% for $T > T_{NI} - 0.5°C$ in the nematic phase.

functions of temperature, from which the indices of refraction were derived using Eq. (11). Next, following the treatment in Ref. [25], the relation

$$Q_B = \frac{\bar{\alpha}}{\Delta\alpha}\frac{n_e^2 - n_o^2}{\bar{n}^2 - 1} \tag{12}$$

was used to find Q_B from the refractive indices. In Eq. (12), $\bar{n}^2 = (n_e^2 + 2n_o^2)/3$, $\Delta\alpha$ represents the anisotropy in molecular polarizability of the perfectly oriented medium, and $\bar{\alpha}$ represents the averaged molecular polarizability. The value of $\bar{\alpha}/\Delta\alpha = 1.84$ in Eq. (12) is taken from Ref. [25], after correction for the HeNe laser wavelength. The results of Karat and Madhusudana are also plotted in Figure 4; the results reported here are in good accord with their earlier measurements [25]. The solid line in Figure 4 represents the L-dG theoretical prediction for $Q_B(T)$, given by

$$Q_B = \frac{b}{2c}\left(1 + \left(1 + \frac{4ac}{b^2}(T - T^*)\right)^{1/2}\right). \tag{13}$$

It is clear from the plot that the L-dG theory does not provide a good quantitative fit of the $Q_B(T)$ curve, so one cannot expect highly accurate quantitative predictions from the extension of L-dG theory to describe

interfacial ordering in the nematic phase. However, within 0.5°C of the N–I transition, the L-dG theory curve overestimates the observed Q_B by less than 10%, so it may be reasonable to expect the L-dG theory to give an accurate qualitative description of the interfacial ordering in the nematic phase near the transition [19].

The results for Sample A are shown in Figures 5–7. In these and subsequent figures, the angle of incidence is chosen just below the first critical angle for total internal reflection at the glass-LC interface. In the isotropic phase, Sample A exhibits complete wetting of the interface by an ordered layer. A plot of the phase shift $\Delta\phi_c$ as a function of the temperature is shown in Figure 5. The strong pretransitional increase of $\Delta\phi_c$ represents the divergence in the thickness of the ordered interfacial region, as predicted by L-dG theory. The solid line in the figure represents a fit to the L-dG theory. It was found to be possible to fit this data with a simpler interfacial free energy than the form shown in Eq. (2); the best fit was obtained with interfacial free energy parameter $g = 3.8 \pm 0.2\,\mathrm{J/m^2}$ and $U = 0$. Chen *et al.* have noted that $\Delta\phi_c$ is proportional to the adsorption parameter Γ in the isotropic phase [5]. According to L-dG theory, the adsorption parameter Γ diverges logarithmically for $Q_0(T_{NI}) > Q_c$, as

$$\Gamma = 2\left(\frac{L}{c}\right)^{1/2} \ln\left(\frac{T_{NI}}{T - T_{NI}}\right). \tag{14}$$

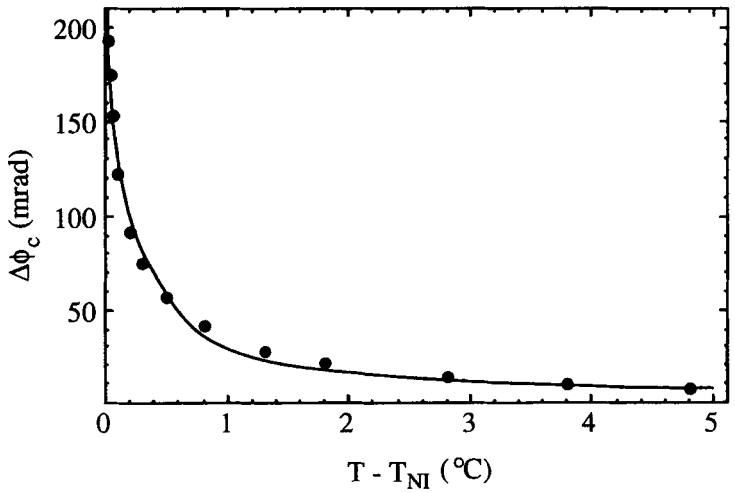

FIGURE 5 Sample A. Isotropic-phase temperature variation of $\Delta\phi_c$. The solid line represents a fit to L-dG theory. In this and subsequent figures, the uncertainty in the phase shift $\Delta\phi$ is ± 0.2 mrad, within the size of the circle used to represent the point.

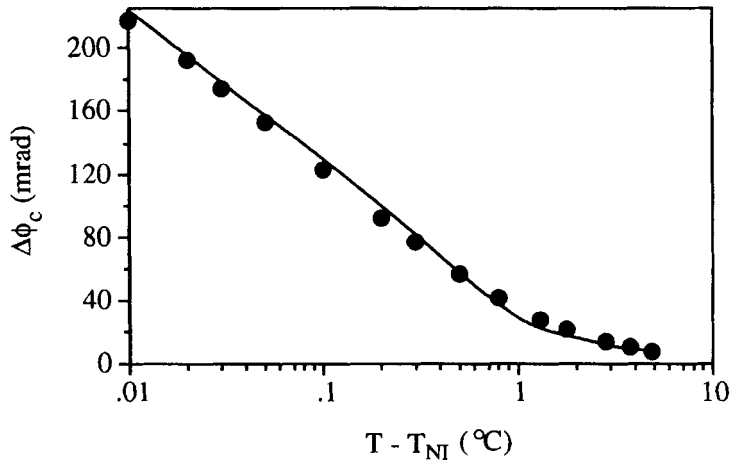

FIGURE 6 Sample A. Isotropic-phase temperature variation of $\Delta\phi_c$. The linearity of the plot verifies the logarithmic divergence predicted by L-dG theory, shown as the solid best-fit line.

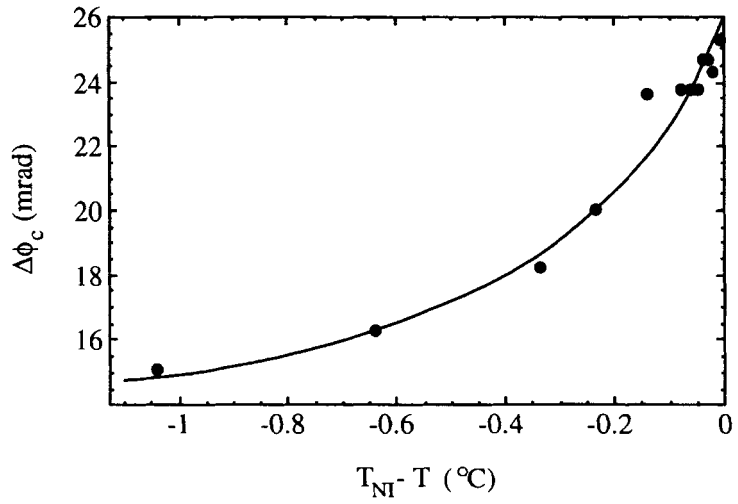

FIGURE 7 Sample A. Nematic-phase temperature variation of $\Delta\phi_c$. The solid line represents a fit to L-dG theory.

The logarithmic nature of the divergence is apparent from the linearity of the plot in Figure 6, where $\Delta\phi_c$ is plotted *vs.* temperature on a semilog scale. The theoretical fit gives $Q_0(T_{NI}) = 0.53 \pm 0.07$, which is larger than $Q_c = 0.37$ as expected for complete wetting. The results in Figures 5, 6 are in accord

with the results for 8CB reported in Ref. [5]. The results for the nematic phase of Sample A are shown in Figure 7. The pretransitional increase of $\Delta\phi_c$ indicates the growth of an interfacial layer with higher order than the bulk nematic, corresponding to partial wetting of the interface. The solid line in the figure represents a fit to the L-dG theory using the same values of the surface free energy parameters g and U used in the isotropic phase.

The results for Sample B are shown Figures 8, 9. In the isotropic phase, the interface in Sample B is wet by an ordered nematic layer whose thickness increases as $T \rightarrow T_{NI}$ but remains finite at T_{NI}, corresponding to partial wetting of the interface by an ordered layer. A plot of the phase shift $\Delta\phi_c$ as a function of the temperature is shown in Figure 8. The pretransitional increase of $\Delta\phi_c$ in the figure represents the growth in the thickness of the ordered interfacial region. The solid line represents a fit to the L-dG theory. The best fit to the isotropic phase data gave $U=0$; the best fit values of the interfacial free energy parameter g is $g=1.10\pm0.05\times10^{-4}\,\mathrm{J/m^2}$. This value of g led to a surface order parameter $Q_0(T_{NI^+}) = 0.09\pm0.01$, which is less than $Q_c=0.37$ as expected for partial wetting. The results for the nematic phase of Sample B are shown in Figure 9. The pretransitional decrease of $\Delta\phi_c$ indicates the growth of an interfacial nematic layer with lower order than the bulk nematic – the interface is partially wet by a disordered layer. The solid line in the figure represents a best fit to the L-dG theory using $g = 1.10\pm0.05\times10^{-4}\,\mathrm{J/m^2}$ and $U=3.0\pm0.3\times10^{-4}\,\mathrm{J/m^2}$, yielding a surface order parameter $Q_0(T_{NI^-}) = 0.07\pm0.01$. It was found that attempts to fit

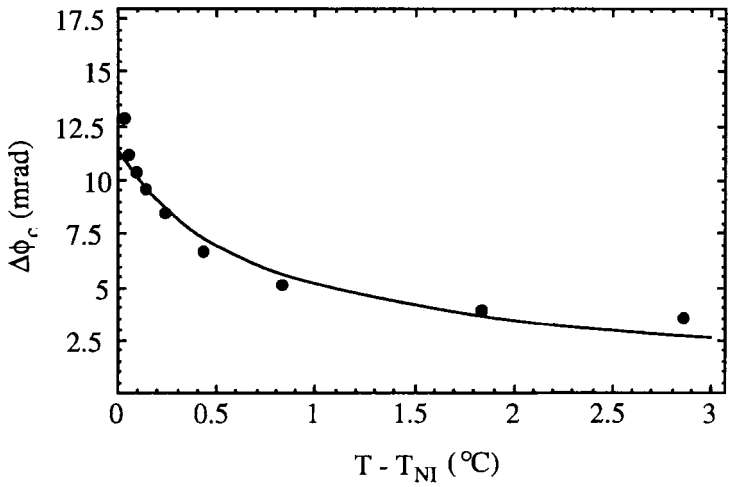

FIGURE 8 Sample B. Isotropic-phase temperature variation of $\Delta\phi_c$. The solid line represents a fit to L-dG theory.

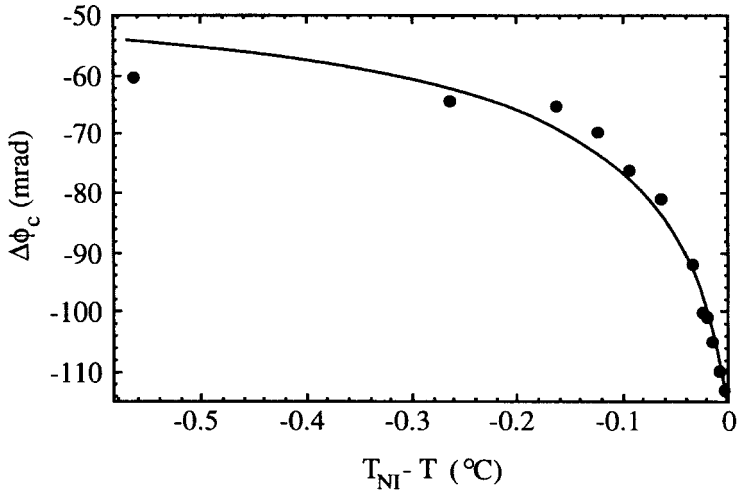

FIGURE 9 Sample B. Nematic-phase temperature variation of $\Delta\phi_c$. The solid line represents a fit to L-dG theory.

the nematic phase data using the same g and U values used to fit the isotropic phase data yielded substantially worse fits, although the qualitative behavior (partial wetting by a disordered nematic surface layer) still resulted. It is unclear why the best-fit values of the surface free energy parameters g and U should differ in the isotropic and nematic phases; the difference probably indicates that the L-dG theory can provide a qualitative, but not quantitative, description of interfacial ordering at the I–N transition.

A brief description of the procedure used to fit the experimental data follows. First, a choice of the surface free energy parameters g and U is made. Next, the surface and bulk order parameters Q_0 and Q_B and the order parameter profile $Q(z)$ are calculated from L-dG theory. Next, using Eq. (12), the profiles of the ordinary and extraordinary indices of refraction $n_o(z)$ and $n_e(z)$ are found. Finally, using the 4×4 matrix method of Berreman, the phase shift $\Delta\phi_c$ is calculated numerically [26]. This calculation is repeated for a series of temperatures T, yielding a theoretical curve $\Delta\phi_c$ *vs.* T.

6. CONCLUSIONS

The qualitative predictions L-dG theory are found to hold consistently in the isotropic and nematic phases of a LC in the vicinity of its I–N

transition. For an interface inducing complete wetting by a nematic layer for $T > T_{NI}$, we find in the nematic phase partial wetting of the interface by a nematic layer of enhanced order. For an interface inducing only partial wetting by a nematic layer for $T > T_{NI}$, we find in the nematic phase partial wetting of the interface by a nematic layer of reduced order. These results are in accord with the predictions of L-dG of theory. One may conclude, then, that the L-dG theory gives a correct qualitative picture of interfacial ordering in LCs, at least in cyanobiphenyls which have been subjected to the most study. Observation of a prewetting transition and complete wetting of the interface by a disordered layer in the nematic phase would be most interesting, completing the catalog of the interfacial ordering behaviors predicted by L-dG theory.

Acknowledgements

This research was supported by grants from Research Corporation and the National Science Foundation–Solid State Chemistry Grant No. DMR93-07350. Technical assistance from Diane Frenster and the gift of the 8CB sample from Dr. Frank Allen at EM Industries are gratefully acknowledged.

References

[1] K. Miyano, *Phys. Rev. Lett.*, **43**, 51 (1979); *J. Chem. Phys.*, **71**, 4108 (1979).
[2] J. Tarczon and K. Miyano, *J. Chem. Phys.*, **73**, 1994 (1980).
[3] H. A. van Sprang, *Mol. Cryst. Liq. Cryst.*, **97**, 255 (1983); *J. Physique*, **44**, 421 (1983).
[4] H. Hsiung, Th. Rasing and Y. R. Shen, *Phys. Rev. Lett.*, **57**, 3065 (1986); *Phys. Rev. Lett.*, **59**, 1983(E) (1987).
[5] W. Chen, L. J. Martinez-Miranda, H. Hsiung and Y. R. Shen, *Phys. Rev. Lett.*, **62**, 1860 (1989); *Mol. Cryst. Liq. Cryst.*, **179**, 419 (1990).
[6] P. Sheng, B. Li, M. Zhou, T. Moses and Y. R. Shen, *Phys. Rev. A*, **46**, 946 (1992).
[7] P. Sheng, *Phys. Rev. Lett.*, **37**, 1059 (1976); *Phys. Rev. A*, **26**, 1610 (1982).
[8] C. A. Croxton, *Mol. Cryst. Liq. Cryst.*, **66**, 223 (1981).
[9] A. Poniewierski and T. J. Sluckin, *Mol. Cryst. Liq. Cryst.*, **111**, 373 (1984); *Mol. Cryst. Liq. Cryst.*, **126**, 143 (1985); *Liq. Cryst.*, **2**, 281 (1987).
[10] T. J. Sluckin and A. Poniewierski, In: Fluid Interfacial Phenomena, Croxton, C. A., Ed. (Wiley, New York, 1986) and references therein.
[11] A. K. Sen and D. E. Sullivan, *Phys. Rev. A*, **35**, 1391 (1987).
[12] D. Beaglehole, *Mol. Cryst. Liq. Cryst.*, **89**, 369 (1982).
[13] S. Immerschitt, T. Koch, W. Stille and G. Strobl, *J. Chem. Phys.*, **96**, 6249 (1992).
[14] H. Kasten and G. Strobl, *J. Chem. Phys.*, **103**, 6768 (1995).
[15] G. P. Crawford and S. Zumer, Eds., Liquid Crystals in Complex Geometries Formed by Polymer and Porous Networks (Taylor and Francis, London, 1995).
[16] C. Bahr, *Intl. J. Mod. Phys. B*, **8**, 3051 (1994) and references therein.
[17] H. Mada and S. Kobayashi, *Appl. Phys. Lett.*, **35**, 4 (1979); *Mol. Cryst. Liq. Cryst.*, **66**, 57 (1981).
[18] J. P. Nicholson, *J. Physique*, **48**, 131 (1987); *J. Physique*, **49**, 2111 (1988).

[19] T. Moses and Y. R. Shen, *Phys. Rev. Lett.*, **67**, 2033 (1991).
[20] S. A. Pikin and E. M. Terent'ev, *Sov. Phys. Crystallogr.*, **33**, 641 (1988).
[21] H. Yokoyama, *J. Chem. Soc. Faraday Trans. II*, **84**, 1023 (1988).
[22] H. Yokoyama, *Mol. Cryst. Liq. Cryst.*, **165**, 265 (1988) and references therein.
[23] The values of a, b and c are derived from H. J. Coles, *Mol. Cryst. Liq. Cryst. Lett.*, **49**, 67 (1978). In Cole's paper, he inappropriately uses values of $\Delta\varepsilon$, the dielectric anisotropy in the nematic phase, given in D. A. Dunmur *et al.*, *Mol. Cryst. Liq. Cryst.*, **45**, 127 (1978), for $\Delta\varepsilon_{max}$, the maximum dielectric anisotropy in perfectly aligned nematic with $Q=1$. Also, Coles' value of Q_c, the nematic order parameter at T_{NI}, is taken from P. P. Karat and N. V. Madhusudana, *Mol. Cryst. Liq. Cryst.*, **40**, 239 (1977). Subsequent to Coles' work, Karat and Madhusudana published a correction to their previously given value for Q_c (see Ref. [25]). Putting corrected numbers into Coles' calculation yields the values of for a, b and c used in this work, which differ from Coles' values by about 20%. For reference, in this work the values $Q_c=0.37$, $\Delta\varepsilon_{max}=0.791$, and $\bar{\varepsilon}=(\varepsilon_{\parallel}+2\varepsilon_{\perp})/3=2.457$ were used (with dielectric values measured at the HeNe wavelength $\lambda=632.8$ nm), derived from the measurements reported in this work and in close agreement with values given in Ref. [25]. Finally, the value used for L is the same as used in previous work in Refs. [6, 7, 19].
[24] F. J. Kahn, *Appl. Phys. Lett.*, **22**, 386 (1973).
[25] P. P. Karat and N. V. Madhusudana, *Mol. Cryst. Liq. Cryst.*, **89**, 249 (1982).
[26] D. Berreman, *J. Opt. Soc. Am.*, **62**, 502 (1971); D. Berreman and T. Scheffer, *Mol. Cryst. Liq. Cryst.*, **11**, 395 (1970).